Full Paper

Journal of the Brazilian Chemical Society

https://dx.doi.org/10.21577/0103-5053.20250168

J. Braz. Chem. Soc. **2026**, *37*, e-20250168, 1-11

PVA Films with Carbonized Kraft Lignin: Physico-Chemical Properties and Application in Gas Detection

Lucas Victor B. V. Fré,[a] *Amanda S. M. de Freitas,*[a] *Jéssica S. Rodrigues,*[b] *André Vitor S. Simões,*[c] *Daniel Komatsu,*[d] *Vinicius Jessé R. de Oliveira,*[c] *Clarissa A. Olivati*[c] *and Marystela Ferreira*[*,a]

[a]*Centro de Ciências e Tecnologia para a Sustentabilidade (CCTS), Universidade Federal de São Carlos (UFSCar), 18052-780 Sorocaba-SP, Brazil*

[b]*Instituto de Ciência e Tecnologia (ICT), Universidade Estadual Paulista (UNESP), 18087-180 Sorocaba-SP, Brazil*

[c]*Departamento de Física, Universidade Estadual Paulista (UNESP), 19060-900 Presidente Prudente-SP, Brazil*

[d]*Departamento de Cirurgia, Faculdade de Ciências Médicas e da Saúde, Pontifícia Universidade Católica de São Paulo (PUC-SP), 18030-070 Sorocaba-SP, Brazil*

Kraft lignin (KL), a major byproduct of the pulp and paper industry, is still largely underutilized, limiting its value in advanced materials. This work investigates whether incorporating carbonized kraft lignin (CKL) into polyvinyl alcohol (PVA) films can enhance their structural and functional properties and enable their use as gas-sensor membranes. PVA films containing 0, 10, 30, and 50 weight percent (wt.%) CKL were prepared and characterized by Fourier-transform infrared spectroscopy (FTIR), X-ray diffraction (XRD), differential scanning calorimetry (DSC), thermogravimetric analysis (TGA), scanning electron microscopy (SEM), water-contact-angle (wettability) measurements, and tensile testing, followed by ammonia (NH_3), ethanol (C_2H_5OH), and toluene (C_7H_8) sensing. CKL increased thermal stability (temperature at 5% mass loss, $T_{5\%}$, up to 135 °C *vs*. 80 °C for neat PVA), raised carbonaceous residue to 15%, and improved Young's modulus while reducing elongation and water contact angle. Gas-sensing tests revealed a strong, reversible current response to NH_3, with PVA/50 wt.% CKL exhibiting the highest current (ca. 23 μA), along with detectable responses to ethanol and toluene. These results demonstrate that CKL is an effective bio-derived additive that upgrades PVA films for sustainable, high-performance gas-sensing applications.

Keywords: polyvinyl alcohol, carbonized Kraft lignin, gas detection

Introduction

Polymeric materials play a pivotal role in modern technology owing to their low density, high mechanical strength, and chemical versatility, enabling the replacement of metals and glass in applications such as automotive components, construction materials, and household products.[1] The long-chain macromolecular architecture of these materials imparts a broad spectrum of optical, electrical, mechanical, and thermal properties that can be precisely tailored for specific applications.[2] Among synthetic polymers, polyvinyl alcohol (PVA) is particularly noteworthy because of its water solubility, semi-conductive character, thermal stability, non-toxicity, and biodegradability.[3-6] These attributes support its widespread use in sensors, energy-storage devices, biomedical scaffolds, filtration membranes, and textile products.

Modification of PVA properties to meet demanding applications is commonly achieved by blending or compounding with other polymers, inorganic fillers, or nanostructured additives to adjust mechanical, thermal, and interfacial behavior.[7,8] A promising renewable modifier is lignin, the second most abundant natural polymer after cellulose, whose aromatic structure

*e-mail: marystela@ufscar.br
Editor handled this article: Adriana Nunes Correia (Associate)

confers rigidity and potential electronic functionality. Kraft lignin (KL), generated as a byproduct of the kraft pulping process, is produced on an industrial scale yet is predominantly burned as a low-value fuel, representing a significant underutilization of a chemically rich resource.[9] Carbonization of KL enhances electrical conductivity and hydrophobic character, yielding carbonized kraft lignin (CKL) with superior thermal stability and structural robustness.[10-12] Incorporation of CKL into PVA offers a sustainable strategy for lignin valorization while producing composite films with enhanced functional properties.

The objective of this study is to develop PVA/CKL composite films containing 0, 10, 30, and 50 wt.% CKL and to evaluate the influence of CKL loading on structural, thermal, mechanical, and surface characteristics. Comprehensive characterization was performed using Fourier-transform infrared spectroscopy (FTIR), X-ray diffraction (XRD), differential scanning calorimetry (DSC), thermogravimetric analysis (TGA), scanning electron microscopy (SEM), contact-angle (wettability) measurements, and tensile testing. In addition, the films were assessed as gas-sensor membranes for the detection of ammonia (NH_3), ethanol (C_2H_5OH), and toluene (C_7H_8) vapors, establishing correlations between CKL content and sensing performance.

Experimental

Materials and reagents

The materials applied for building the films were: the polyvinyl alcohol (PVA), $[–CH_2CHOH–]_n$, molecular weight of 104500.0 u (NEON). The lignin comes as byproduct of paper processing through the kraft process, provided by the paper company Suzano, located in São Paulo State, Brazil. The KL is originated from *Eucalyptus urograndis*.[1] Previous studies[2,3] characterized the lignin used in this work, the gel permeation chromatography presented an average molar mass (M_w) of 4025 ± 209 g mol^{-1} of glycerol PA, and molecular weight 92.10 u (Anidrol).

Methods

The process started by carbonizing the KL in a muffle furnace under nitrogen atmosphere, from room temperature to 1000 °C at a heating rate of 5 °C min^{-1}, held at 1000 °C for 2 h and then cooled naturally to room temperature.[4,5] The lignin powder became carbon foam during the process, and it was ground and sieved using a 100-mesh screen. 1 g of PVA was dissolved in 30 mL of water in a heating plate with magnetic stirring until boiling and complete solubilization of the PVA pallets, then 1 mL of glycerol was added in the solubilized PVA, as a crosslinking agent.[6] The solution was poured on a 70 mm glass Petri dish plate and taken to the oven at 60 °C with vacuum pressure of 211 mmHg for 10 h to dry the water. For the other films, the same procedure was followed, except by adding different portions of CKL, being 10, 30, and 50 wt.% of PVA, during the dissolving PVA process.

Structural characterization

Structural characterization was conducted using several groups of analysis described in the following paragraphs. Analyses had three repetitions as standard and presented the PVA film as control film for comparing. Some analyses differ in size and number of repetitions, specified in the analysis description.

The atomic interactions were analyzed through Fourier transform infrared spectroscopy (FTIR) on a Nicolet Summit IR 200 FT-IR instrument in attenuated total reflectance (ATR) mode, using 128 scans, nominal resolution of 4.0 cm^{-1}, in the range of 4000 to 400 cm^{-1}. The spectra were obtained in the Ominic Paradigm (Thermo Scientific, USA).

X-ray diffraction (XRD) experiments indicated the modifications in the semi-crystalline structure of polymeric matrix. The equipment was a Bruker diffractometer (Model D8 Discovery; Cu Kα, λ 0.15418 nm). The spectra were taken with a 0.05 step, an exposure time of 3 s, a voltage of 40 kV, and a current of 30 mA.

Thermal measurements were also conducted using differential scanning calorimetry (DSC) to study the stability of films in a Q10 model from TA Instruments, USA, equipped with an RCS 40 cooling system. The samples were heated from 25 to 350 °C with a heating rate of 20 °C min^{-1}. All measurements were performed under a nitrogen flow of 50 mL min^{-1}, and the sample mass was maintained at around 4-7 mg. Thermal events were identified and calculated during the second heating scan, supported by the TRIOS® software.

The surface modifications were studied through micrographs obtained by a scanning electron microscope, JEOL, 1200 EX II. Energy beam at 10 kV, working distance of 11 mm.

Wettability was studied using the sessile drop technique in a Ramé Hart goniometer (model 100-00), with deionized water. For each sample, three water droplets have been deposited on different surface points, each with 10 contact angle measurements. Results correspond to the average of 10 measurements.

Mechanical properties of the samples were determined

using an Emic 23-30 universal testing machine, with a 500 N load cell. A stretching rate of 10 mm min^{-1}, a temperature of 25 °C and a total of 5 samples were equally presented. The films were prepared, following the ASTM D882-97.23,[7] through dimensioning 100 mm × 15 mm.

Application for a gas sensor

Sensory measurements were performed through the study of current *versus* time (I *vs*. t) curves. Nitrogen (N_2) gas was used as an inert baseline to stabilize the sample. The N_2 also pushes the gas over the sample, favoring the interaction of gas and the substrate. This interaction occurs in a saturation regime and is repeated in cycles of 1 min of interest gas and 2 min of N_2, in a stable flow of 60 normal liters *per* hour (60 N L h^{-1}) in a chamber. A constant voltage of 2 V was applied to the device using a Keithley 238 SMU DC power source under controlled temperature conditions of 23 °C. The electrode consists of an interdigitated electrode (IDE) made of gold. The samples, dimensioning 10 × 40 mm, were placed over the electrode and closes the circuit to study the current through it as described by Bittencourt *et al*.[8]

Results and Discussion

Structural characterization

Figure 1 presents the FTIR spectra of PVA, PVA/CKL films, and CKL samples (Figure 1a), highlighting the differences in relevant chemical groups, as well as the XRD patterns (Figure 1b), which illustrate the effect of CKL on the crystallinity of the PVA matrix.

The FTIR spectra, presented by Figure 1a, revealed changes among the films as the CKL content increases. The neat PVA film (red curve) exhibits a broad and intense band centered at ca. 3300 cm^{-1}, assigned to the O–H stretching of hydroxyl groups involved in strong hydrogen bonding.[9] This high intensity is expected for PVA plasticized with water and glycerol, which increases hydroxyl availability. In contrast, the CKL spectrum (black curve) does not display this band, reflecting the low hydroxyl group content in carbonized kraft lignin, resulting from the removal of most oxygenated groups during the carbonization process. In the composites (blue = 10% CKL, pink = 30% CKL, green = 50% CKL), a subtle progressive decrease in the intensity of this band is observed as the CKL content increases, indicating a reduction in the availability of free hydroxyl groups. In the 50% CKL film, the peak becomes significantly attenuated, evidencing a pronounced hydrophobization effect and strong PVA-CKL interactions. This trend is consistent with the increased water contact angle previously observed for these films.

In the region around 2925 cm^{-1}, doublets are present in all samples, corresponding to the C–H stretching of CH_2 groups.[10] The similarity in the profile of this band among the curves confirms that the aliphatic backbone of the PVA matrix remains preserved and that CKL is well-dispersed, without significant alteration of the primary chain structure.[11]

A pronounced band at ca. 1710 cm^{-1}, attributed to C=O stretching of carbonyl groups from residual acetate groups in PVA, is clearly visible in the neat polymer. In the composites, this band gradually decreases with increasing CKL content, with the most marked reduction in the 50% CKL film. This attenuation suggests the formation of specific intermolecular interactions-likely hydrogen bonding-between residual hydroxyl groups in PVA and oxygen-containing moieties in CKL, promoting reorganization within the polymer matrix.[12]

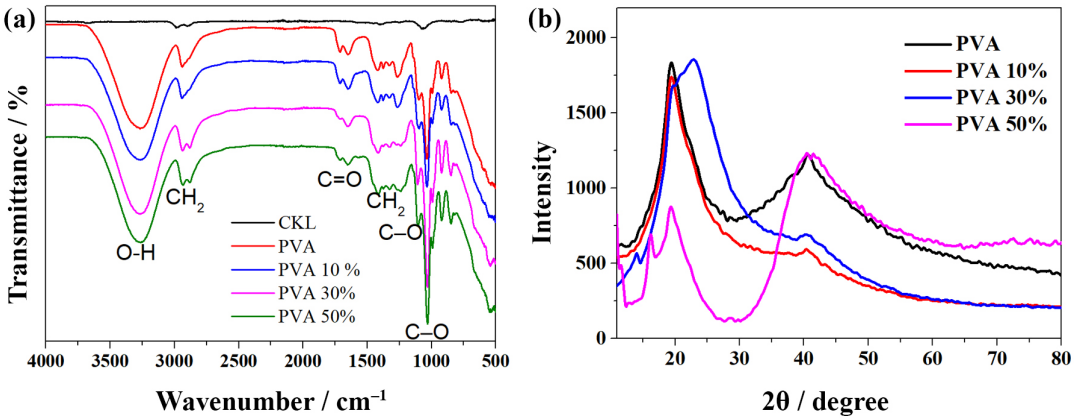

Figure 1. (a) Fourier transform infrared spectroscopy (FTIR-ATR) spectra from the polyvinyl alcohol (PVA) film, carbonized kraft lignin (CKL) powder, and PVA/CKL in the proportions of 10, 30, and 50% film ratios. (b) X-ray diffraction (XRD) curves of the PVA film and CKL in the proportions, 10, 30, and 50% films. It compares the influence of lignin in different ratios in the material polymeric net structure. The plot presents peaks at 2θ = 14°, 17°, 20°, and 40° which fade as the ratio of lignin increases.

In the fingerprint region (1500-500 cm^{-1}), neat PVA presents intense peaks at 1396 cm^{-1} (CH_2 bending), 1239 cm^{-1} (C–O stretching in secondary alcohols and C=C skeletal vibrations)[13] and 1026 cm^{-1} (C–O stretching sensitive to crystallinity).[14] These bands lose intensity and, in some cases, broaden as the CKL content increases, indicating interference with chain packing and crystallinity due to the amorphous and aromatic character of CKL. In the 50% CKL composite, the band at 1026 cm^{-1} becomes less defined, consistent with reduced crystallinity and increased structural disorder in the matrix.

The CKL spectrum exhibits few and low-intensity bands, which is typical of carbonized lignin, where the predominance of condensed aromatic domains and the scarcity of C–H and C–O bonds result in low infrared absorption.[4] This profile reinforces the role of CKL as a hydrophobic, carbon-rich filler that interacts with PVA mainly through physical interactions and limited hydrogen bonding, rather than through a high density of polar functional groups.

The analysis of XRD reveals changes in the structural parameters of the films. Polymers are typically semi-crystalline materials, characterized by regions of dense atomic organization that diffract X-rays and define their unique structure. Figure 1b presents the XRD patterns for both PVA and PVA with different ratios of CKL films. The CKL was not analyzed. The compound does not present a crystalline structure, since the monolignols (lignin monomers) that compose its structure are too irregular to form a periodic atomic pattern.[15] The lignin compound is formed by 30 different monomers varying the rate and presence of monolignols from the wood it was extracted.[16]

The pure PVA polymer exhibits two proponent peaks: one at 2 $\theta \approx 20°$, representing the semi-crystalline nature of the polymer, and a smaller, broader peak around $2\theta \approx 40°$,[17,18] other minor peaks might also be seen before $2\theta \approx 20°$, however, their exposure depends on random distribution of powder material or preferential orientation of material, when studied film forms. All the three modified films with CKL retain those major peaks, indicating that the semi-crystalline structure is preserved. The PVA film and the PVA10% had almost the same intensity at this peak however the other films presented different behavior. The PVA30% suffered an enlargement, which can be justified by the presence of lignin as an interstitial matter.[19] The PVA50% suffered the major modifications, compared to the PVA film, the intensity of signal reduced, also being explained by the presence of lignin and another important point is the film analysis which might benefit one planar density than other. Yet, the films PVA30% and PVA50% have shown minor peaks at $2\theta \approx 15$ and 17°, respectively.[20] These peaks are natural from the PVA structure, not caused by CKL. The presence or absence of peaks that are characteristic of the material in the study is justified due to the XRD analysis. The reflected planar density of minor peaks might be covered by noise signal and film position.

The addition of CKL affects the X-ray diffraction pattern by introducing new atomic bonds, as shown in the FTIR analysis. While the characteristic peaks remain at their original positions, the peak at $2\theta = 20°$ decreases in intensity. This reduction suggests that CKL particles may physically cover and reduce the X-ray reflection in this dense region. Conversely, the peak around $2\theta = 40°$ increases in intensity, not due to increased reflection from the lignin, but rather due to noise introduced by the CKL, which enhances the apparent intensity of this peak. New peaks are not revealed in any CKL modified film, confirming that the CKL has no crystallinity to add in the material and affects just the intensity and width due to formation of new atomic bonds.

The PVA/CKL film microstructures differ from PVA film microstructure, impacting the wettability behavior. The wettability analysis is important to study the material behavior towards aqueous solutions and water exposure. Table 1 shows the wettability expressed by the droplet contact angle upon PVA and PVA/CKL films. The contact angle < 90° indicates the material surface hydrophilic feature, being 33.09°. When the film is in contact with water, it absorbs the droplet, swelling the surface confirming its hydrophilic nature. Such properties make pure PVA suitable as an additive to enhance hydrophilicity in composite materials. In contrast, the carbon lignin inserted into the polymeric matrix makes the film more hydrophobic, once lignin itself presents hydrophobic feature.[21] However, the wettability study performed showed otherwise. The CKL modified films enhanced hydrophilic behavior, being the PVA10% CKL film 27.66º, the PVA30% CKL film 26.73º, and the PVA50% CKL film 24.64º. These values indicate that the CKL was involved by the film structure and not present on the surface. Bringing back the FTIR analysis, it is possible to observe that the presence of surface hydroxyl groups is still, regarding the amount of CKL added in the film. The intensity of the –OH band present in the FTIR spectra for the PVA/CKL sample when compared to the PVA films, corroborated with the increase of hydrophilicity.

Table 1. Results of the deionized water wettability test for the polyvinyl alcohol (PVA) film and PVA modified with 10, 30, and 50 wt.% carbonized kraft lignin composites

Wettability / degree			
PVA	PVA10%	PVA30%	PVA50%
33.09 ± 0.82	27.66 ± 2.52	26.73 ± 2.47	24.64 ± 2.33

Yet, considering the statistical test one way *T*-test presented by Figure S1 (Supplementary Information section), adding CKL significantly changes the behavior of film wettability. Between the treatments 10 and 30% there is no significant difference, either between 30 or 50%.

Another studied feature enhanced through the modification of PVA film with CKL is the thermal characteristics of the PVA/CKL film. TGA (Figure 2a) and first derivative of thermogravimetric (DTG) curves (Figure 2b) display parameters such as $T_{5\%}$ (onset temperature of degradation corresponding to a 5% mass loss), T_{max} (temperature at the maximum mass loss rate), Δ_m (mass loss rate up to T_{max}), and $R_{900°C}$ (carbonaceous residue at 900 °C), which are summarized in Table 2.

Table 2. Results of thermogravimetric analyses for the test for the polyvinyl alcohol (PVA) film and PVA modified with 10, 30, and 50 wt.% carbonized kraft lignin composites

Sample	$T_{5\%}$[a] / °C	T_{max}[b] / °C	Δ_m[c] / %	$R_{900°C}$[d] / %
PVA	80	273	52	0.2
PVA10%	108	274	53	0.4
PVA30%	74	276	44	8.5
PVA50%	135	275	37	15.3

[a]Onset temperature of degradation with a 5% mass loss; [b]temperature at the maximum mass loss rate; [c]mass loss rate until T_{max}; [d]carbonaceous residue at the end of the degradation process in 900 ºC.

The results reveal a clear influence of CKL concentration on the thermal stability of the films. The $T_{5\%}$ value, indicative of the onset of degradation, increased from 80 °C (PVA) to 108 °C (PVA10%), and reached 135 °C (PVA50%), suggesting that CKL acts as a thermal barrier that delays early decomposition events. Interestingly, PVA30% showed a slight decrease in $T_{5\%}$, possibly due to incomplete dispersion or local heterogeneities. The CKL may act as a physical or chemical barrier that delays the initial volatilization of PVA components, resulting in slightly improved thermal resistance.[22]

The T_{max} values remained relatively constant across the samples (273-276 °C), indicating that the temperature at which maximum degradation occurs is less sensitive to CKL concentration. However, the Δ_m decreased steadily with increasing CKL content, from 52% (PVA) to 37% (PVA50%), showing that CKL inhibits thermal decomposition and promotes char formation. The most striking trend was observed in the $R_{900°C}$, which rose from 0.2% (PVA) to 15.3% (PVA50%). This significant increase in residual mass confirms the formation of a stable carbonaceous structure from CKL, which remains after thermal degradation. The increasing residue correlates with the greater presence of thermally resistant aromatic structures from CKL.[23] These findings highlight that CKL improves the thermal robustness of PVA films, particularly at higher loadings. This behavior is attributed to both physical shielding effects and possible chemical interactions that reduce chain mobility and promote char stabilization.

The DSC curves (Figure S2, Supplementary Information section) reveal multiple thermal transitions influenced by CKL content. All samples show a broad endothermic event between 50-150 °C, more pronounced in PVA10% and less intense in PVA50%, associated with the loss of absorbed water and partial relaxation of amorphous regions in the polymer matrix. This region can include the glass transition temperature (Tg) of PVA, particularly when moisture is present, as water acts as a plasticizer and reduces Tg values.[24]

The most prominent endothermic peaks appear in the 250-320 °C range and are attributed to the thermal degradation of PVA and possible transitions associated with CKL decomposition.[4,12] For the pure PVA film, a peak is observed around 275-280 °C, whereas for CKL-containing

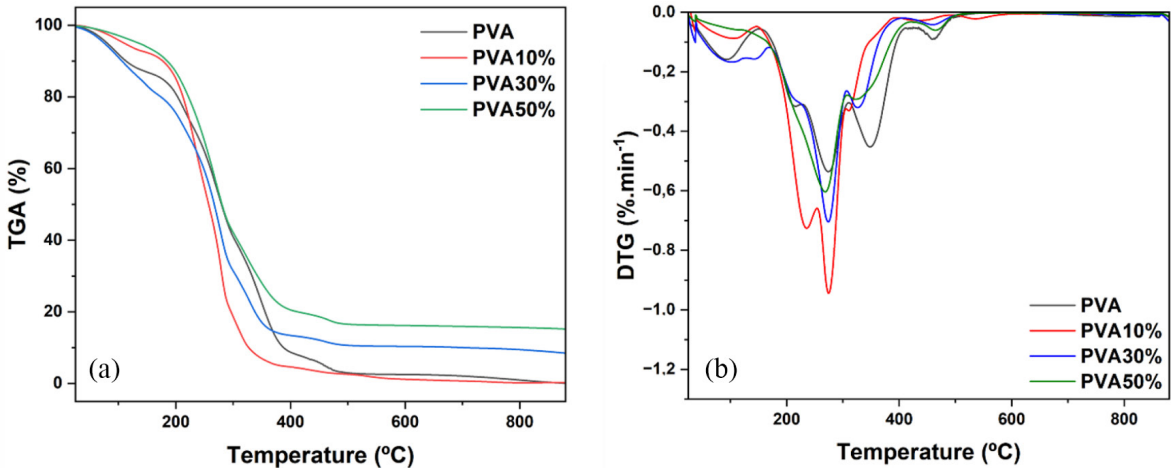

Figure 2. (a) Thermogravimetric analysis (TGA) curves, (b) first derivative of thermogravimetric (DTG) curves for the polyvinyl alcohol (PVA) film and PVA modified with 10, 30, and 50 wt.% carbonized kraft lignin composites.

samples (PVA10%, PVA30%, and PVA50%), this event is shifted to higher temperatures, with PVA50% showing the broadest and most delayed peak. This indicates that CKL increases the thermal resistance of the system.

This stabilization can be explained by the barrier effect and strong interactions between PVA chains and aromatic domains in the carbonized lignin, which restrict chain mobility and delay volatilization or decomposition. Moreover, the presence of thermally stable graphitic and aromatic carbon structures in CKL reduces the intensity and sharpness of the endothermic transitions due to energy dissipation through char formation.[12]

The broadening and intensity reduction of these transitions with increasing CKL content is consistent with the formation of a more crosslinked and restricted network, which resists thermal flow and transition. These results align with the TGA and DTG data, confirming that CKL acts as an effective thermal stabilizer in the PVA.[25]

In summary, the DSC analysis demonstrates that increasing CKL content in PVA films (*i*) shifts degradation and melting-related events to higher temperatures, (*ii*) reduces the intensity of thermal transitions, and (*iii*) broadens the heat flow signals. These changes reflect a more thermally stable and structurally constrained matrix, making the material more suitable for thermally demanding applications.

The modification of chemical bonds and atomic positioning in the semi-crystalline structure between PVA and PVA/CKL ratios indicates potential differences in film surface structure, which were analyzed through SEM micrographs. SEM provides detailed visualization of the surface morphology of the materials. The micrographs in Figure 3 illustrate the surface features of the films and materials studied. Figures 3a and 3b show the surface morphology of the pure PVA film, which exhibits a reticular pattern formed during the solubilization and drying processes. This process results in a regular film structure, as seen in the magnified view of the reticular pattern in Figure 3b. Figure 3c presents the lowest ratio of CKL in the film. It is possible to observe that the film has no longer uniform surface, forming cracks on the surface. Figure 3d highlights the surface of PVA10%, showing fragments of CK, by the shining grains on the structure, that contributes to its characteristic morphology.

Figures 3e and 3f show the surface morphology of the PVA30% composite film. The SEM micrographs reveal two distinct regions on the surface, indicating a heterogeneous distribution of CKL within the PVA matrix. In Figure 3e, the surface is predominantly formed by a continuous PVA layer, typical of the drying process, which produces a smooth and narrow film structure. However, disruptions

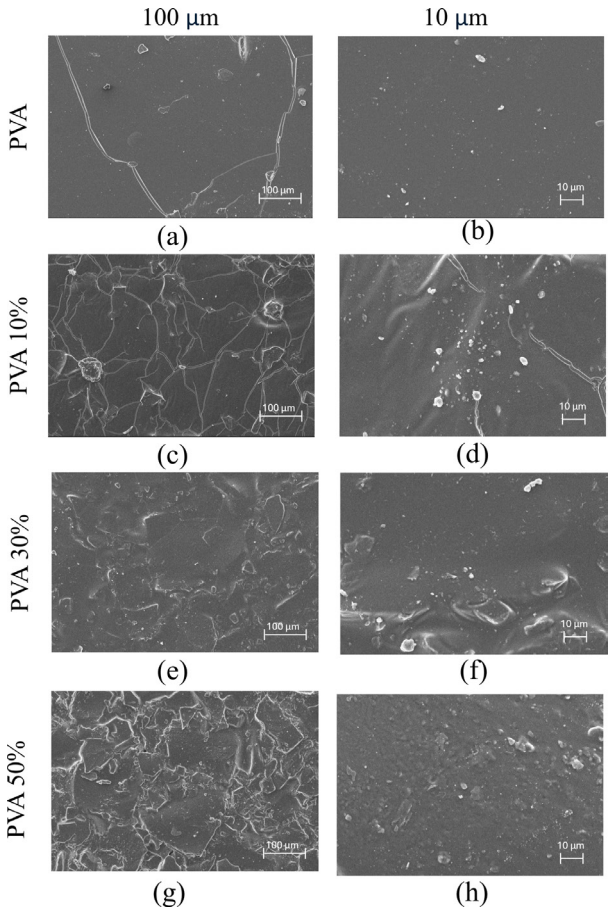

Figure 3. Micrographs of polyvinyl alcohol (PVA) and composites of PVA and carbonized kraft lignin (CKL) in different ratios, being (a) the PVA film magnification of ×200, and (b) the polyvinyl alcohol (PVA) film in higher magnification, ×1,000. (c) The first ratio of carbonized kraft lignin (CKL) being the treatment polyvinyl alcohol modified with 10 wt.% carbonized kraft lignin (PVA 10%), ×200, (d) a higher magnification, given evidence on the CKL powder (e) presents the treatment polyvinyl alcohol modified with 30 wt.% carbonized kraft lignin (30% PVA), magnification of ×200, (f) higher magnification, ×1,000, showing the distortion in the surface, (g) the treatment (polyvinyl alcohol modified with 50 wt.% carbonized kraft lignin) 50% PVA, magnification of ×200, and (h) presents higher magnification, ×1,000, that is possible to observe a granular surface over and underneath the polymer matrix.

in this surface, such as torn or rifted regions, expose underlying structures where CKL is present. Figure 3f provides a closer look at these rifted areas, revealing CKL particles embedded within the matrix. These particles are more concentrated in the exposed regions, suggesting that CKL tends to aggregate beneath the surface layer of PVA rather than being evenly distributed across the film. The formation of these two regions can be explained by the differences in physical and chemical properties between PVA and CKL. CKL, being more hydrophobic and rigid due to its carbonized structure, interacts less uniformly with the hydrophilic PVA matrix during the drying process, leading to partial phase separation and the observed dual morphology.

This heterogeneous morphology highlights the composite nature of the PVA/CKL film, where CKL particles are integrated within the PVA matrix but not uniformly distributed. Such a structure is essential to the overall properties of the composite, as CKL enhances thermal stability and mechanical strength, while PVA provides flexibility and favors processing.

Figure 3g shows how 50 wt.% CKL affected the structure of material. It is possible to observe that the CKL influenced the PVA solidification, forming scales on the surface of material. This uneven structure on surface might influence the wettability of the substrate, since the material has greater superficial area than the more homogeneous films. Figure 3h also shows grains on the material, however, we can see that the spots are not lighted up. It indicates that the material is covered with a thin layer of PVA, since the conductive material on surface would have been brighter.

After the addition of CKL to PVA at concentrations of 10, 30, and 50%, an increase in Young's modulus values was observed compared to the pure PVA sample. This increase can be attributed to the strong interactions between PVA and KL particles.[26] Moreover, the uniform distribution of CKL particles within the PVA matrix may further contribute to this enhancement, as well-dispersed CKL particles can create more hydrogen bonds between PVA and KL, increasing the Young's modulus of the PVA/CKL samples in comparison to pure PVA.[27]

Figure 4 illustrates the Young's modulus values as a function of CKL content in PVA. According to Al Kiey *et al.*,[28] the Young's modulus of pure PVA was 341.20 MPa. Lo Faro *et al.*[29] reported a value of 740.40 MPa, while Dong *et al.*[30] found a value of 250.00 MPa. In the present study, the pure PVA sample exhibited a significantly lower Young's modulus of 1.14 MPa. This reduction can be attributed to the presence of glycerol, which acts as a plasticizer and decreases the rigidity of the PVA matrix.

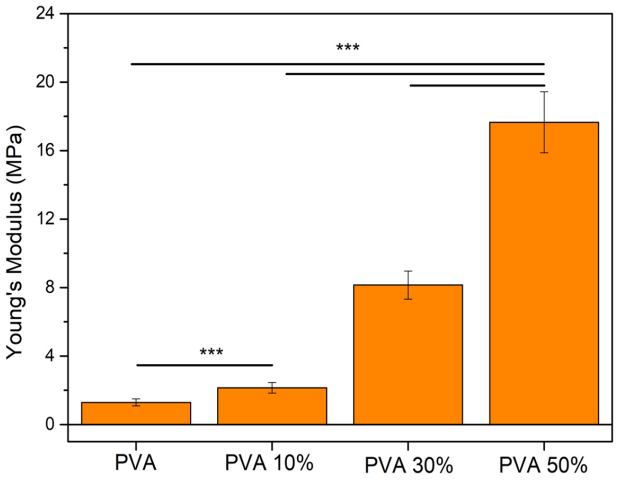

Figure 4. Young's modulus as a function of the carbonized kraft lignin content in polyvinyl alcohol with carbonized kraft lignin modifications in weight percentage (10, 30, and 50%) (***$p < 0.001$).

Figure 5 illustrates the elongation at break values as a function of KL content in PVA. According to Li *et al.*,[31] pure PVA exhibited an elongation at break of 176.00%. Similarly, Awad and Khalaf[32] reported a value of 68.72%. In the present study, the pure PVA sample showed a significantly higher elongation at break of 680.80%. This substantial increase is attributed to the presence of glycerol in the formulation, which acts as a plasticizer, enhancing the flexibility and extensibility of the PVA matrix.

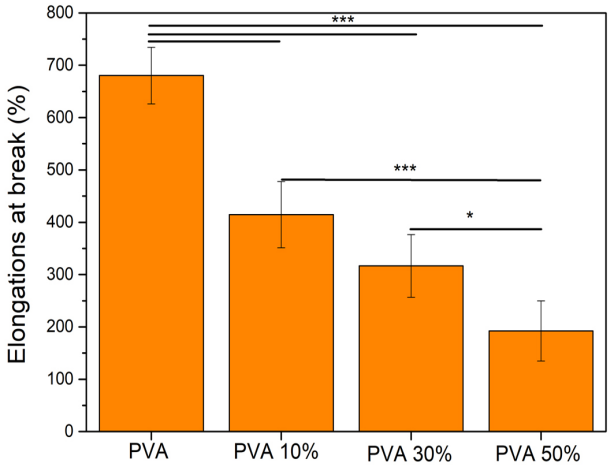

Figure 5. Elongation at break as a function of the carbonized kraft lignin content in polyvinyl alcohol with carbonized kraft lignin modifications in weight percentage (10, 30, and 50%) (*$p < 0.05$ and ***$p < 0.001$).

After the addition of CKL to PVA at concentrations of 10, 30, and 50%, a decrease in elongation at break values was observed compared to the pure PVA sample. This behavior can be attributed to the formation of strong hydrogen bonds between CKL and PVA, which enhance interfacial adhesion and promote uniform CKL dispersion within the PVA matrix. Additionally, the presence of CKL increases the density of the film, thereby reducing its flexibility. Consequently, these factors contribute to the reduced deformability of the PVA/CKL samples in comparison to the pure PVA.[33]

Application for a gas sensor

The characterization of films show how CKL ratios influenced the structure of PVA film. After characterization, the films were tested as gas sensors for ammonia, ethanol, and toluene gases. Figure 6 summarizes all the tests; Figure 6a shows the interaction between PVA film with the three gases, where it was possible to see that, when exposed to ammonia gas in a

saturation regime, PVA film exhibits a reversible change in its electrical current, showing an interaction between the material and the analyte. The interaction outcome low current. The other tested gases did not present the same behavior. The PVA, exposed to toluene, did not present irreversible interaction. The analysis started with an exponential shrink overtime. Ethanol gas slightly increased the current in the initial seconds of each cycle, but overall, the current shrunk throughout the analysis.

The PVA 10% film, Figure 6b, also showed a reproducible response to ammonia, resulting in higher current peaks, compared to the PVA film. The first cycle resulted in a reduced current that stabled at 7.5 µA. For toluene gas, at the first cycle, it is possible to see an irreversible attachment between gas and subtract, as previously noticed between the gas and PVA film. Ethanol gas had the same behavior as PVA film, differing only in the higher current.

The PVA 30% film, Figure 6c, ammonia gas interaction was similar to the PVA/CKL10%, even at the current values, however, the other gases presented better reversibility. The toluene gas interaction presented saturation throughout the analysis, where one can see the last two cycles presented almost the same current as N_2 push. Ethanol interaction was again the one with lowest current, in this CKL ratio it became possible to observe the reversibility of interaction of gas and subtract, saturating only the last cycle.

The last treatment, PVA 50% (Figure 6d), also presented a reversible interaction with ammonia vapor, this represents the highest current interaction in the analysis, 23 µA, being 200 times higher than the initial PVA film. The ethanol gas interaction also had the best performance about current peak and in this CKL ratio, also this treatment had no saturation, being dragged out during N_2 flow. The toluene gas interaction is partially saturated, presenting shrunk current value in each cycle.

The sample was evaluated in cycles of 3 min, alternating between exposure to target gas vapor and nitrogen, with a continuous flow of 60 normal liters *per* min (60 N L min^{-1}). During the tests, the sensor demonstrated stability by returning to the initial electrical current when exposed to nitrogen vapor, while it exhibited a significant increase in current when exposed to the target gas vapor, confirming its positive response to the gas. Furthermore, it was observed that the material maintained its functionality for at least five consecutive cycles of saturation and remained reusable for weeks after the first test, indicating promising durability. It is also possible to see that the result is reproducible, maintaining similar peak current values between most

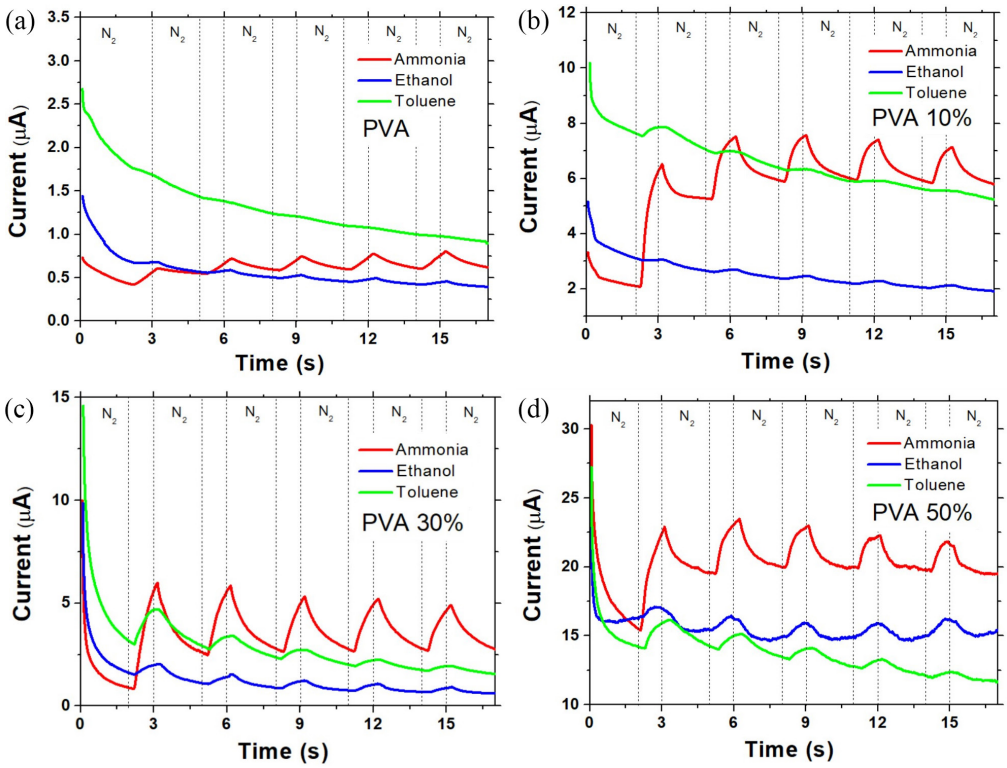

Figure 6. Gas detection test for ammonia, ethanol and toluene which sorted in (a) polyvinyl alcohol (PVA) results, (b) polyvinyl alcohol modified with 10 wt.% carbonized kraft lignin (PVA10%), (c) polyvinyl alcohol modified with 30 wt.% carbonized kraft lignin (PVA30%) and (d) polyvinyl alcohol modified with 50 wt.% carbonized kraft lignin (PVA 50%). Repeated cycles of 1 min of interest gas and 2 min of N_2, in a stable flow of 60 normal liters *per* hour (60 N L h^{-1}), tension of 2 V.

treatments (30 and 50%) The current increases along with the amount of CKL. Ammonia gas was detected in all treatments, however, neither ethanol nor toluene present clear current throughout cycling. Toluene gas presents shrinking current responses for all treatments throughout each cycle, which can be attributed to the fact that the sensitive material is still in its initial state, allowing for greater efficiency in oxidation/reduction reactions or swelling of the polymer chains. Table 3 shows a comparative of other works that applied lignin-based modifications to detect ammonia vapor. It summarizes the polymeric matrix, the modification, potential, and the average current. Conductive polymer sensors rely on the variation of material resistance from gas and material interaction, thus setting the potential input, that does not vary, the output of current indicates the variation.[34] The greater variations of current requite less sensible devices, decreasing costs.

During these initial cycles, the diffusion has not yet fully permeated the active layer of the sensor. In subsequent cycles, a gradual decrease in the emitted current is observed, a behavior that can be attributed to mechanisms such as reduced gas diffusion due to a more saturated surface or structural changes, such as compaction, caused by the continuous contact between toluene vapor and the sensitive material. Despite this reduction in intensity over the cycles, the sensor maintains a consistent response format in its reductions, demonstrating its functional reproducibility for PVA50% CKL. The interaction between PVA and ammonia occurs through hydrogen bonding, leading to a swelling and a change in chain conformation. This interaction is facilitated by the presence of hydroxyl groups in PVA that can form hydrogen bonds with ammonia molecules.[38-40]

Conclusions

The experimental results confirm that incorporating CKL into PVA films markedly improves their structural, thermal, and sensing performance. The key findings of the films developed include a rise in the onset degradation temperature ($T_{5\%}$) from 80 °C for neat PVA to 135 °C for the 50 wt.% CKL film, an increase in carbonaceous residue at 900 °C to 15%, and a significant enhancement of mechanical strength (higher Young's modulus with reduced elongation at break). Gas-sensing tests demonstrated that CKL addition substantially improves detection capability, with the PVA/50 wt.% CKL composite exhibiting the highest and reversible NH_3 current response (ca. 23 μA) and measurable responses to ethanol and toluene. These outcomes corroborate the initial hypothesis that CKL acts as a sustainable additive, providing thermal stability, mechanical reinforcement, and superior gas-sensing sensitivity, thereby validating the proposed strategy for valorizing kraft lignin in advanced, biodegradable sensor materials.

Supplementary Information

Supplementary information (regarding the wettability results presented as a box plot and the differential scanning calorimetry (DSC) curves of polyvinyl alcohol and the composites of polyvinyl alcohol with 10, 30, and 50 wt.% carbonized kraft lignin treatments) is available free of charge at http://jbcs.sbq.org.br as PDF file.

Data Availability Statement

The raw data is available to in the repository github: https://github.com/lfre-cloud/PVA-Films-with-Carbonized-Kraft-Lignin-Physico-chemical-Properties-and-Application-in-Gas-Detection.git. Any additional data may be obtained from the corresponding authors upon request.

Acknowledgments

We thank the "Programa de Pós-Graduação em Ciência dos Materiais - PPGCM-So" for availability of XRD equipment - Shimadzu 6100.

This work was funded by FAPESP - 2023/06505 (MF), 2023/17363-0 (ASMF) and 2023/00335-4 (JSR); CAPES - 88887.803614/2023-00 (LVBVF), INEO FAPESP 2014/50869-6, and FINEP 01.22.0179.00 (MARTMA).

Table 3. Current outcomes of ammonia vapor detection considering different polymeric matrixes and lignin-based materials

Polymer matrix	Material	Tension / V	Average current	Reference
PVA	lignin	2	23 μA	this work
PLA	gold-decorated lignin nanoparticles	2	0.1 nA	35
PVA	polyaniline	2	10 μA	8
Polyurethane foam	lignin with graphene oxide	2	36 mA	36
PVA	polypyrrole (PPy) doped with dodecylbenzene sulfonic acid	2	150 nA	37

PVA: polyvinyl alcohol; PLA: polylactic acid; PPy: polypyrrole.

Author Contributions

L. V. B. V. F. was responsible for conceptualization, data curation, formal analysis, investigation, visualization, and writing (original draft, review and editing); A. S. M. F. and J. S. R. for conceptualization, data curation, formal analysis, validation and writing; D. K., A. V. S. S., and V. J. R. O. for data curation, formal analysis and writing; C. A. O. for supervision, resources, and writing, review and editing; M. F. for conceptualization, methodology, project administration, supervision, resources, and writing, review and editing.

References

1. Rodrigues, J. S.; de Freitas, A. S. M.; Maciel, C. C.; Mendes, S. F.; Diment, D.; Balakshin, M.; Botaro, V. R.; *Ind. Crops Prod.* **2023**, *191*, 115948. [Crossref]
2. Araújo, L. C. P.; Yamaji, F. M.; Lima, V. H.; Botaro, V. R.; *Bioresour. Technol.* **2020**, *314*, 123757. [Crossref]
3. Rodrigues, J. S.; Lima, V.; Araújo, L. C. P. A.; Botaro, V. R.; *Ind. Eng. Chem. Res* **2021**, *60*, 10863. [Crossref]
4. Rodrigues, J. S.; de Freitas, A. D. S. M.; Maciel, C. C.; Guizani, C.; Rigo, D.; Ferreira, M.; Hummel, M.; Balakshin, M.; Botaro, V. R.; *Int. J. Biol. Macromol.* **2023**, *240*, 124460. [Crossref]
5. Rao, G.-S.; Nabipour, H.; Zhang, P.; Wang, X.; Xing, W.; Song, L.; Hu, Y.; *J. Mater. Res. Technol.* **2020**, *9*, 4655. [Crossref]
6. Tathimongkon, J.; Chaijaruwanich, A.; Nakkiew, W.; Wattanutchariya, W.; *Adv. Sci. Technol*. **2024**, *143*, 27. [Crossref]
7. ASTM 882-97: *Standard Test Method for Tensile Properties of Thin Plastic Sheeting*, ASTM, 2018. [Link] accessed in October 2025
8. Bittencourt, J. C.; de Santana Gois, B. H.; Rodrigues de Oliveira, V. J.; da Silva Agostini, D. L.; de Almeida Olivati, C.; *J. Appl. Polym. Sci.* **2019**, *136*, 47288. [Crossref]
9. Ma, X.; Yu, J.; *Starch/Stärke* **2004**, *56*, 545. [Crossref]
10. Yan, P.; Xu, Z.; Zhang, C.; Liu, X.; Xu, W.; Zhang, Z. C.; *Green Chem.* **2015**, *17*, 4913. [Crossref]
11. Rynkowska, E.; Fatyeyeva, K.; Marais, S.; Kujawa, J.; Kujawski, W.; *Polymers* **2019**, *11*, 1799. [Crossref]
12. Monteiro, V. A. C.; da Silva, K. T.; da Silva, L. R. R.; Mattos, A. L. A.; de Freitas, R. M.; Mazzetto, S. E.; Lomonaco, D.; Avelino, F.; *React. Funct. Polym.* **2021**, *166*, 104980. [Crossref]
13. Kumar, A.; Negi, Y. S.; Bhardwaj, N. K.; Choudhary, V.; *Adv. Mater. Lett.* **2013**, *4*, 626. [Crossref]
14. Cao, J.; Xiao, G.; Xu, X.; Shen, D.; Jin, B.; *Fuel Process. Technol.* **2013**, *106*, 41. [Crossref]
15. Goudarzi, A.; Lin, L.-T.; Ko, F. K.; *J. Nanotechnol. Eng. Med.* **2014**, *5*, 021006. [Crossref]
16. Ralph, J.; Lapierre, C.; Boerjan, W.; *Curr. Opin. Biotechnol.* **2019**, *56*, 240. [Crossref] [PubMed]
17. Ricciardi, R.; Auriemma, F.; de Rosa, C.; Lauprêtre, F.; *Macromolecules* **2004**, *37*, 1921. [Crossref]
18. Patel, A. K.; Bajpai, R.; Keller, J. M.; *Microsyst. Technol.* **2014**, *20*, 41. [Crossref]
19. Rodríguez-Mirasol, J.; Cordero, T.; Rodríguez, J. J.; *Carbon* **1996**, *34*, 43. [Crossref]
20. Bhat, N. V.; Nate, M. M.; Kurup, M. B.; Bambole, V. A.; Sabharwal, S.; *Nucl. Instrum. Methods Phys. Res. B* **2005**, *237*, 585. [Crossref]
21. Zhao, X.; Xiong, D.; Liu, Y.; *J. Mech. Behav. Biomed. Mater.* **2018**, *82*, 27. [Crossref] [PubMed]
22. El Moustaqim, M.; El Kaihal, A.; El Marouani, M.; Men-La-Yakhaf, S.; Taibi, M.; Sebbahi, S.; El Hajjaji, S.; Kifani-Sahban, F.; *Sustainable Chem. Pharm.* **2018**, *9*, 63. [Crossref]
23. Vannarath, A.; Thalla, A. K.; *J. Cleaner Prod.* **2021**, *325*, 129263. [Crossref]
24. Gómez, I.; Otazo, E. M.; Hernández, H.; Rubio, E.; Varela, J.; Ramírez, M.; Barajas, I.; Gordillo, A. J.; *Polym. Degrad. Stab.* **2015**, *112*, 132. [Crossref]
25. Nazrin, A.; Sapuan, S. M.; Zuhri, M. Y. M.; Ilyas, R. A.; Syafiq, R.; Sherwani, S. F. K.; *Front Chem.* **2020**, *8*, 213. [Crossref]
26. Ye, D.; Jiang, L.; Hu, X.; Zhang, M.; Zhang, X.; *Int. J. Biol. Macromol.* **2016**, *83*, 209. [Crossref]
27. Ramadhan, M. H.; Nurrahman, A.; Steven, S.; Mardiyati, Y.; *Emergent Mater.* **2024**, *8*, 2231. [Crossref]
28. Al Kiey, S. A.; Soliman, T. S.; Taha, M.; Khalid, A.; *Mater. Chem. Phys.* **2024**, *323*, 129644. [Crossref]
29. Lo Faro, E.; Park, K.; Sadeghi, K.; Fava, P.; Seo, J.; *Prog. Org. Coat.* **2024**, *197*, 108799. [Crossref]
30. Dong, M.; Bilotti, E.; Zhang, H.; Papageorgiou, D. G.; *Int. J. Biol. Macromol.* **2025**, *295*, 139545. [Crossref]
31. Li, X.; Liu, Y.; Ren, X.; *Int. J. Biol. Macromol.* **2022**, *216*, 86. [Crossref] [PubMed]
32. Awad, S. A.; Khalaf, E. M.; *J. Thermoplast.-Compos. Mater.* **2020**, *33*, 69. [Crossref]
33. Phansamarng, P.; Bacchus, A.; Hassan Pour, F.; Kongvarhodom, C.; Fatehi, P.; *Ind. Crops Prod.* **2024**, *221*, 119217. [Crossref]
34. Lakkis, S.; Younes, R.; Alayli, Y.; Sawan, M.; *Sens. Rev.* **2014**, *34*, 24. [Crossref]
35. Papa, P.; Luciani, G.; Grappa, R.; Venezia, V.; Guerriero, E.; Serrecchia, S.; De Cesare, F.; Zampetti, E.; Taddei, A. R.; Macagnano, A.; *Sensors* **2025**, *25*, 3536. [Crossref]
36. Rodrigues, J. S.; de Freitas, A. S. M.; de Lima, L. F.; Lopes, H. S. M.; Maciel, C. C.; Fré, L. V. B. V.; Pires, A. A. F.; de Lima, V. H.; Oliveira, V. J. R.; Olivati, C. A.; Ferreira, M.; Riul, A.; Botaro, V. R.; *Int. J. Biol. Macromol.* **2024**, *268*, 131883. [Crossref] [PubMed]
37. Gois, B. H. S.; Bittencourt, J. C.; David-Parra, D. N.; de Almeida Olivati, C.; Merlini, C.; da Silva Agostini, D. L.; *Mat. Res.* **2021**, *24*, e20210031. [Crossref]

38. Anju, V. P.; Jithesh, P. R.; Narayanankutty, S. K.; *Sens. Actuators, A* **2019**, *285*, 35. [Crossref]
39. Singhal, A.; Kaur, M.; Dubey, K. A.; Bhardwaj, Y. K.; Jain, D.; Pillai, C. G. S.; Tyagi, A. K.; *RSC Adv.* **2012**, *2*, 7180. [Crossref]
40. Trebs, I.; Meixner, F. X.; Slanina, J.; Otjes, R.; Jongejan, P.; Andreae, M. O.; *Atmos Chem. Phys.* **2004**, *4*, 967. [Crossref]

Submitted: August 13, 2025
Final version online: November 5, 2025